Graphene at fluidic interfaces

Belyaeva, L.A.

CHAPTER 4

Contact angle measurement of freestanding square millimeter single layer graphene

Square millimeters of free-standing graphene do not exist per se because of thermal fluctuations in two-dimensional (2D) crystals and their tendency to collapse during the detachment from the substrate. Here, millimeter-scale freely suspended graphene is formed by injecting an air bubble underneath a graphene monolayer floating at the water-air interface, which allowed us to measure the contact angle on fully free-standing non-contaminated graphene. A captive bubble measurement shows that free-standing clean graphene is hydrophilic with a contact angle of 42°±3°. The proposed design provides a simple tool to probe and explore the wettability of 2D materials in free-standing geometries and will expand our perception of 2D materials technologies from microscopic to now millimeter-scales.

This chapter was published as an article: Anna V. Prydatko*, Liubov A. Belyaeva*, Lin Jiang, Lia M.C. Lima and Grégory F. Schneider, Nat.Comm., 2018, 9, 4185.

4.1. Introduction

The wetting properties of graphene have been a subject of intensive theoretical and experimental investigations over the last decade. Extremely thin and electrically conductive, graphene is widely used in biosensors, lab-on-a-chip and microfluidics platforms where graphene is in contact with water, vapor and analytes.[1–4] Although graphene was long believed to be a graphite-like material,[5–7] some recent studies have shown a wide spread of water contact angle (CA),[5,6,8–10] with values ranging from 10° when supported by water[10] to 127° on solid substrates.[5] One reason for such discrepancies in the values of the contact angle is the difference in sample preparation and measurement conditions.[6,8] The adsorption of airborne hydrocarbons, the cleanliness and quality of the graphene/substrate and graphene/water interface can have significant effects on the measured contact angles, which, however, can be minimized in most cases by conducting experiments in controlled atmospheres and by avoiding the use of polymers during the transfer process.[11–14]

The wetting characteristics of a material are dictated by both the surface and the bulk properties of the material, which implies the impossibility to determine the intrinsic wetting properties of two-dimensional (2D) materials which have no bulk. In other words, all wetting characteristics of graphene, such as contact angle and surface energy, refer not only to the graphene surface but also to the bulk phase underneath it and must not be regarded as solely graphene's properties.

In this respect, probing the wetting characteristics of free-standing graphene can give an indispensable insight for understanding the wettability of graphene. Yet, due to the extreme fragility of graphene and other 2D materials, studies on free-standing graphene have been limited to theoretical predictions with only a few experimental works on partially suspended graphene.[15,16] Being the only experimental indication of the wettability of free-standing graphene up to now, the contact angle of partially suspended graphene is still an indirect measure and requires multistep sample preparation which may result in an ill-defined graphene-substrate interface yielding a range of contact angle values.

In this work the wettability of free-standing graphene is directly characterized using a simple and clean captive bubble methodology. The captive bubble method, i.e. the injection of an air bubble underneath graphene floating on water, allows for the formation of a graphene free-standing area as large as 1.5 by 1.5 mm, the largest free-standing area that has been reported so far for a 2D material. Essentially, graphene remains floating on the water surface after copper etching, intrinsically preventing any transfer or handling-related contamination and corrugation. An additional advantage is that the graphene side on which the contact angle is measured (i.e. the side that initially faces copper and then water) has never been exposed to ambient air and is therefore not subjected to airborne hydrocarbons adsorption.[16,17]

4.2. Results

4.2.1. Captive bubble versus sessile drop

The captive bubble method measures the contact angle using an air bubble at a solid/liquid interface. Often, the method works best for hydrophilic substrates in which liquid spreads out yielding more difficulties to determine the contact angle with the sessile drop technique, e.g. for contact lenses and hydrogels.[19,20] The captive bubble and sessile drop configurations represent the same three-phase equilibrium and, therefore, are equivalent in determining the contact angle values (Figure 4.1a, b).

The difficulties associated with the contact angle measurement on free-standing graphene are that 2D materials do not withstand the mechanical disturbances originating from – for example – depositing a droplet of liquid on their surface because of their extremely low thickness.[10] Additionally, free-standing graphene as big as a macroscopic droplet does not exist. Instead, using the captive bubble geometry (i.e. a water-air bubble-graphene interface), allows for a reliable contact angle measurement. The advantage of this method in comparison to the sessile drop technique is that deionized water is primarily composed of water molecules (and therefore less contamination per volume percent compared to air

and vacuum; i.e., water protects graphene from airborne hydrocarbon contamination). Another remarkable advantage of the technique is that the bubble is saturated with water vapor, therefore yielding a contact angle in equilibrium in time.

For the comparison of the captive bubble method with the sessile drop technique the water contact angle was first measured on highly oriented pyrolytic graphite (HOPG). For that, HOPG was exfoliated with a scotch tape in air or in water depending on the method used for measuring the contact angle. The average contact angles were 59°±3° for the sessile drop method and 60°±3° for the captive bubble method (Figure 4.1 a, b). Both methods show high reproducibility on solid substrates.

Additionally, contact angles of graphene with a 300 nm layer of poly(methyl methacrylate) (PMMA) were measured using the captive bubble method and the sessile drop technique as control tests respectively. Graphene appeared wetting transparent in both cases displaying the contact angle of the bare PMMA support – that is 53°±4° measured by the captive bubble method (Figure 4.1c) and 54°±3° using the sessile drop method (Figure 4.1d). Noteworthy, after two days the graphene/PMMA sample became more hydrophobic and after six days the contact angle of graphene increased up to 85° (Figure 4.1d). Such transition from a hydrophilic to a hydrophobic surface is known to be caused by the adsorption of hydrocarbons from the air.[11] A surface energy analysis using the Owens-Wendt method (see Appendix 3) showed that while the graphene surface is clean, hydrocarbons tend to adsorb to minimize the free surface energy. The decrease of the total surface energy and its dispersive component is consistent with previous reports (Figure 4.1e).[21]

The agreement between the sessile drop and captive bubble results for freshly-exfoliated graphite and graphene/PMMA in which graphene was not exposed to air shows that, although the air in the bubble may contain hydrocarbon contaminants, they do not affect the contact angle because of the short-lived graphene-bubble contact and/or negligible amount of hydrocarbons present in the bubble.

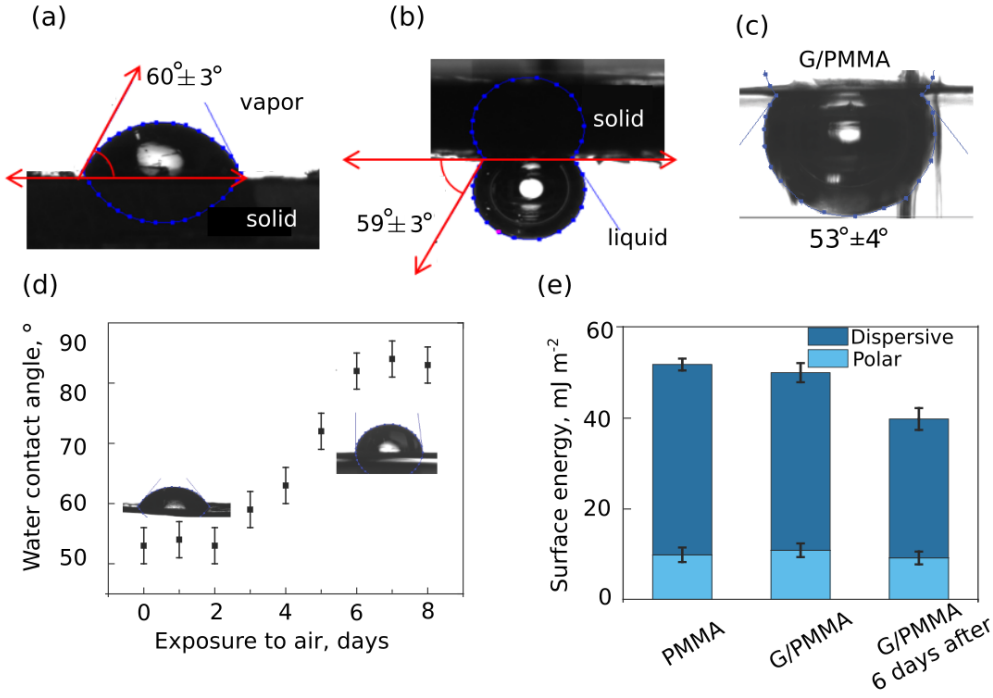

Figure 4.1. Sessile drop and captive bubble measurements on graphite and supported graphene. a) Sessile drop of water on freshly exfoliated highly oriented pyrolytic graphite (HOPG) in air. The measured contact angle is 60°±3°. The measurement was reproduced on ten samples and the error bar represents the standard deviation. b) Captive bubble configuration on freshly exfoliated HOPG in water. The measured contact angle is 59°±3°. The measurement was reproduced on ten samples and the error bar represents the standard deviation. c) Captive bubble measurement of water contact angle on graphene supported by a poly(methyl methacrylate) (PMMA) layer. The measurement was reproduced on ten samples and the error bar represents the standard deviation. d) Sessile drop contact angle measurement of graphene supported by a PMMA layer constantly exposed to air as a function of air exposure time. The measurement was reproduced on three samples and the error bar represents the standard deviation. e) Surface energies and polar and dispersive components of the surface energy for PMMA, graphene supported by PMMA and graphene supported by PMMA which was exposed to air for six days. The measurement was reproduced on three samples and the error bar represents the standard deviation.

4.2.2. Captive bubble method to study graphene. Inflection of floating graphene

For contact angle measurement on graphene using the captive bubble technique, an air bubble is deposited using an inverted needle underneath graphene (Figure 4.2a,b; for technical details on the sample preparation and contact angle measurements see Methods in Appendix 3). From the optical image one can see that the area of graphene surrounded by air on both sides is 1.5 by 1.5 mm large, the largest free-standing graphene area ever reported (Figure 4.2c).

However, due to its extreme flexibility and thinness, graphene inflects above the surface of water under the pressure of the air bubble and the inflection should be taken into account for the calculation of the contact angle. For flexible materials, forces at the three-phase contact line cannot be described by Young equation, as it is for flat rigid substrates. Instead, numerous investigations of the contact angle show that the force balance on soft materials is best described by Neumann's triangle.[22–28] According to Neumann's theory the total contact angle on a deformed substrate can be described as a sum of two angles, beneath and above the contact line, i.e. $\theta_{above} + \theta_{below}$ (Figure 4.d). Since the angle measured in the captive bubble method is the contact angle between the air bubble and the solid, i.e. θ_{air}, the water contact angle should be recalculated as $180° - \theta_{air}$. Taking into consideration the inflection of graphene, the contact angle of water on deflective graphene is therefore $180° - (\theta_{above} + \theta_{below})$ (Figure 4.d).

The measurements of the contact angle of an air bubble on graphene, thus, are more complex than measuring the contact angle of a drop of water on graphene, and consist of measuring the contact angle measurement above and below the three-phase contact line. The schematics and optical image of an example of a water the contact angle measurement water on graphene are shown in Figure 4.2e and 4.2f respectively. The results show that graphene is hydrophilic with a contact angle of water of 42°±7° (Figure 4.2f).

Interestingly, a smaller bubble causes a decrease of the measured angle $180° - \theta_{below}$ and of the inflection angle θ_{above}, but the difference between the two, i.e. the actual contact angle, is independent of the bubble volume and equal to

42°±3°: for a bubble volume of 6µl, the resulting contact angle is 42° (i.e. the difference between the measured angle of 56° and the inflection angle of 14°), and for a bubble volume of 0.2 µl, the measured angle is 42° and there is no observable inflection to account for as the smaller bubble does not induce significant stretch in the graphene sheet (Figure 4.f, g). These observations are in agreement with other reported works and hypothesis that the size-dependence of the contact angle occurs only on rough and heterogeneous surfaces and not on smooth homogeneous surfaces like graphene.[29–31]

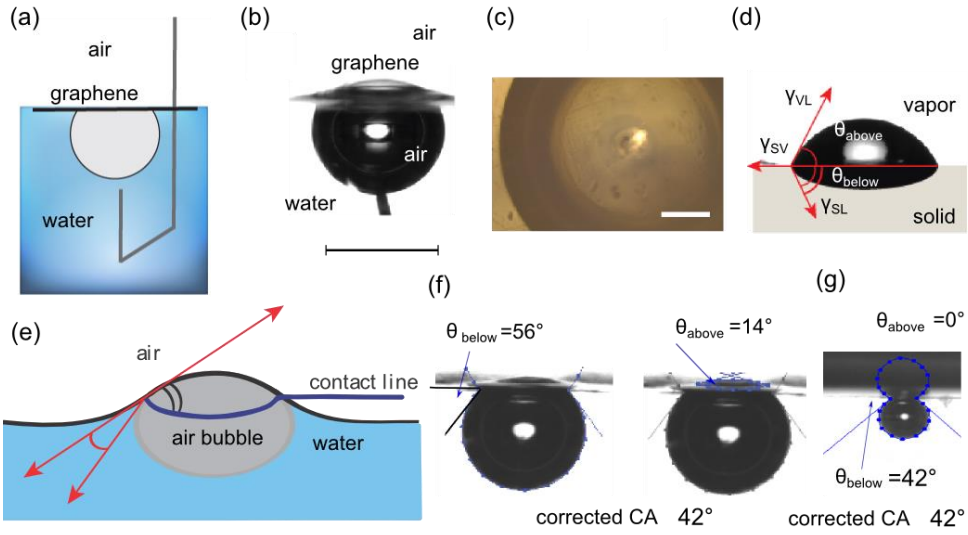

Figure 4.2. Captive bubble configuration for measuring the contact angle of water on free-standing graphene. a) Schematic illustration of the captive bubble setup for measuring the contact angle of water on free-standing graphene. b) Optical image of graphene on top of an air bubble (side view). Scale bar represents 2 mm. c) Optical image of graphene suspended above the air bubble (top view). Scale bar represents 500 µm. d) Geometry of the contact line on a soft elastic substrate. The contact angle of three phases is a sum of angles below ($\boldsymbol{\theta}_{below}$) and above ($\boldsymbol{\theta}_{above}$) the horizontal line. e) Neumann's triangle. Surface energy balance for captive bubble on graphene. f) Optical images of a captive bubble on graphene and calculation of the contact angle for an inflected graphene with an air bubble of 6 µl. g) Optical image of a captive bubble on graphene and calculation of the contact angle (bubble volume 0.2 µl)

4.2.3. Few-layer graphene and modified graphene

Multilayered graphene (bi- and four-layer) did not exhibit appreciable difference in the water contact angle (Figure 4.3a). Since defects and chemisorption of atomic hydrogen/oxygen on graphene are known to affect wetting,[32] contact angles of graphene modified with H_2 and O_2 plasma were also measured (Figure 4.3a, see Methods in Appendix 3 for details on plasma treatment). After modification with H_2 plasma the contact angle on graphene-on-copper decreased from 76°±5° to 68°±5° which can be explained by the cleaning effect of the plasma (Raman characterization of graphene before and after the modification, Figure A3.3 in Appendix 3).[33,34] No difference in the wettability of suspended graphene after the surface modification with a H_2 plasma was observed. Separately, an air bubble on graphene modified by a O_2 plasma was very unstable and tended to slip away from the graphene which could be explained by oxygen functionalities induced by the O_2 plasma.[35] Overall, contact angle values of modified and multilayer graphene are similar to the contact angle of monolayer pristine graphene given the error margins (Figure 4.a).

4.2.4. Effect of humidity

Recently graphene has been shown to turn hydrophilic when floating on water due to the wetting transparency effect.[10,36] In order to test the effect of the environment on one side of graphene on its hydrophobicity on the other side, experiments under different humidities were performed. Contact angles of water using the captive bubble method were measured at the humidities of 98%, 85% and 50% regulated by saturated salt solution of K_2SO_4 and KCl (see Methods in Appendix 3 for more details).[37] Interestingly, a higher humidity level yields lower water contact angle: 29°±8° at 98%, 34°±7° at 85% and 42°±7° at 50% humidity (Figure 4.3b).

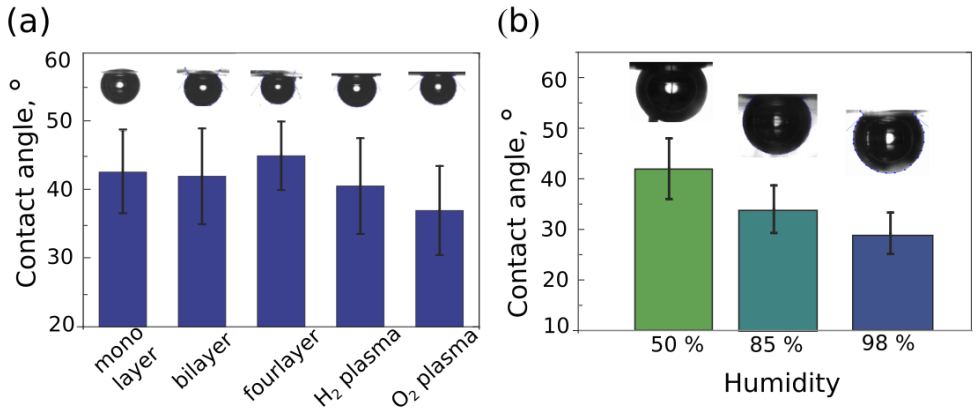

Figure 4.3. Graphene contact angles measured by the captive bubble method. a) Contact angles of water on free-standing, monolayer, bilayer, four-layer graphene and graphene modified with H_2 and O_2 plasma, measured using the captive bubble method. The measurement was reproduced on five samples and the error bar represents the standard deviation. b) Contact angle of water on free-standing graphene in 50%, 85% and 98% relative humidity. The measurement was reproduced on two samples and the error bar represents the standard deviation.

As for all microscopic approaches, the captive bubble method is technically challenging for studying 2D materials because they are fragile and even small vibrations can break them apart. In some cases cracks and holes appear on the graphene surface during the etching process[15] which can prevent an air bubble from staying underneath the graphene. Furthermore, CVD (chemical vapor deposition) grown graphene is not monocrystalline and has grain boundaries which could make graphene permeable to air.[38,39] In our experiments the air bubble underneath graphene was stable from two seconds up to fifteen minutes after which either the bubble or graphene would collapse (Figure A3.4 in Appendix 3 for optical images before and after the captive bubble experiment). The main sources of the degradation of graphene quality when floating on water were the high rate of copper etching, vibrations, intense air circulation and, partly as a result of all the aforementioned, movability of the graphene on the surface of water. In fact, the quality and stability of the floating graphene was significantly improved by using a less concentrated etchant solution of ammonium persulfate (0.3M and lower), or by minimizing vibrations and air circulations, and, importantly, immobilizing graphene with a lipid clamp (see

Methods in Appendix 3 for more details on the lipid clamp and sample preparation).[40]

4.3. Discussion

Although partly suspended graphene on a texturized substrate shows hydrophobic properties with contact angle up to 85°,[15,16] our findings demonstrated that clean fully free-standing graphene is mildly hydrophilic (with a measured water contact angle of 42°, in agreement with theoretical predictions on the hydrophilicity of graphene with contact angle of water ranging from 37° to 44°[11,17,41]). However, such low contact angle is rather surprising, because given the wetting transparency of graphene[9,10], the contact angle of free-standing graphene should be identical to the contact angle of air, i.e. 180°. The wetting behavior, therefore, in this case cannot be only dictated by the transmission of air-water interactions, but is substantially affected by the phenomena occurring at the graphene surface. Remarkably, the measured contact angle values for mono-, bi-, four layer graphene and graphene treated with O_2 and H_2 plasma are similar (Figure 4.a), also supporting this assumption. The hydrophilicity of graphene (i.e., the fact that water wets free-standing graphene) could be explained by the formation of π-hydrogen bonding between water molecules and the aromatic system, as it is for benzene-water interaction.[42,43] Another hypotheses attributes the hydrophilicity of graphene to the spontaneous adsorption of OH^- ions on graphene surfaces[44] which could lead to interactions with water and an increase of the repulsive double layer interaction between air (in the bubble) and graphene. As a complementary evidence for the hydrophilic behavior of graphene in water, stable surfactant-free dispersions of graphene have been recently obtained in degassed water.[44,45] The apparent inability of graphene to form stable aqueous dispersions, which was previously attributed to the hydrophobicity of graphene, is now explained by the adsorption and further coalescence of nanobubbles on the graphene surface.

On the other hand, an increase in the environment humidity, i.e. the concentration of water molecules on the top side of graphene, leads to a decreasing water contact angle value and therefore an increase in the

hydrophilicity of graphene (Figure 4.b), indicating that the transparency of graphene to water-water interactions still has a substantial contribution in addition to the water-graphene interactions mentioned above.

In conclusion, a millimeter-sized suspended 2D material was obtained by simply harvesting surface tension forces at the air-water-graphene-air interface using an air bubble captivated on graphene floating on water. Direct contact angle measurements have shown that free-standing graphene has hydrophilic properties. Advantageously to other methods, the captive bubble technique allows to probe the water/graphene/air interface, in the cleanest way, avoiding any irregularities arising from the transfer and handling processes. The observed hydrophilicity could be explained by the formation of hydrogen bonds which would impact the spontaneous adsorption of water on the graphene surface.
This work provides a stimulus to further study the still unexplored basic properties of suspended 2D materials, such as their surface chemistry, surface energy, compressive and flexural strength and device interaction at a millimeter scale in a free-standing geometry.

4.4. References

1. Shuo, S. *et al.* Graphene-based microfluidics for serial crystallography. *Lab Chip* **16,** 3082–3096 (2016).

2. Mirsaidov, U. *et al.* Scrolling graphene into nanofluidic channels. *Lab Chip* **13,** 2874–2878 (2013).

3. Chang, J., Zhou, G., Christensen, E. R., Heideman, R. & Chen, J. Graphene-based sensors for detection of heavy metals in water: a review. *Anal. Bioanal. Chem.* **406,** 3957–3975 (2014).

4. Dan, Y., Lu, Y., Kybert, N. J., Luo, Z. & Johnson, A. T. C. Intrinsic response of graphene vapor sensors. *Nano Lett.* **9,** 1472–1475 (2009).

5. Taherian, F., Marcon, V., Van Der Vegt, N. F. A. & Leroy, F. What is the contact angle of water on graphene? *Langmuir* **29,** 1457–1465 (2013).

6. Raj, R., Maroo, S. C. & Wang, E. N. Wettability of graphene. *Nano Lett.* **13,** 1509–1515 (2013).

7. Shin, Y. J. *et al.* Surface-energy engineering of graphene. *Langmuir* **26,** 3798–3802 (2010).

8. Wang, S., Zhang, Y., Abidi, N. & Cabrales, L. Wettability and surface free energy of graphene films. *Langmuir* **25,** 11078–11081 (2009).

9. Rafiee, J. *et al.* Wetting transparency of graphene. *Nat. Mater.* **11,** 217–222 (2012).

10. Belyaeva, L. A., van Deursen, P. M. G., Barbetsea, K. I. & Schneider, G. F. Hydrophilicity of graphene in water through transparency to polar and dispersive interactions. *Adv. Mater.* **30,** 1–7 (2018).

11. Li, Z. *et al.* Effect of airborne contaminants on the wettability of supported graphene and graphite. *Nat. Mater.* **12,** 925–931 (2013).

12. Kozbial, A., Gong, X., Liu, H. & Li, L. Understanding the Intrinsic Water Wettability of Molybdenum Disulfide (MoS_2). *Langmuir* **31,** 8429–8435 (2015).

13. Kozbial, A., Zhou, F., Li, Z., Liu, H. & Li, L. Are graphitic surfaces hydrophobic? *Acc. Chem. Res.* **49,** 2765–2773 (2016).

14. Aria, A. I. *et al.* Time evolution of the wettability of supported graphene under ambient air exposure. *J. Phys. Chem. C* **120,** 2215–2224 (2016).

15. Ondarçuhu, T. *et al.* Wettability of partially suspended graphene. *Sci. Rep.* **6,** 24237 (2016).

16. Zhao, Y. *et al.* Investigations on the wettability of graphene on a micron-scale hole array substrate. *RSC Adv.* **6,** 1999–2003 (2016).

17. Yiapanis, G., Makarucha, A. J., Baldauf, J. S. & Downton, M. T. Simulations of graphitic nanoparticles at air-water interfaces. *Nanoscale* **8,** 19620–19628 (2016).

18. Li, J. & Wang, F. Water graphene contact surface investigated by pairwise potentials from force-matching PAW-PBE with dispersion correction. *J. Chem. Phys.* **146,** (2017).

19. Read, M. L., Morgan, P. B., Kelly, J. M. & Maldonado-Codina, C. Dynamic contact angle analysis of silicone hydrogel contact lenses. *J. Biomater. Appl.* **26,** 85–99 (2011).

20. Lin, M. C. & Svitova, T. V. Contact lenses wettability in vitro: effect of surface-active ingredients. *Optom. Vis. Sci.* **87,** 440–447 (2010).

21. Kozbial, A. *et al.* Study on the surface energy of graphene by contact angle measurements. *Langmuir* **30,** 8598–606 (2014).

22. Style, R. W. *et al.* Universal deformation of soft substrates near a contact line and the direct measurement of solid surface stresses. *Phys. Rev. Lett.* **110,** 1–5 (2013).

23. Lubbers, L. A. *et al.* Drops on soft solids: free energy and double transition of contact angles. *J. Fluid Mech.* **747,** (2014).

24. Metois, J. J. Elastic straining of a thin graphite layer by a liquid droplet or a non-epitaxed Pb crystallite. *Surf. Sci.* **241,** 279–288 (1991).

25. Jerison, E. R., Xu, Y., Wilen, L. A. & Dufresne, E. R. Deformation of an elastic substrate by a three-phase contact line. *Phys. Rev. Lett.* **106,** 1–4 (2011).

26. Hui, C.-Y. & Jagota, A. Deformation near a liquid contact line on an elastic substrate. *Proc. R. Soc. A Math. Phys. Eng. Sci.* **470,** 20140085 (2014).

27. Style, R. W. & Dufresne, E. R. Static wetting on deformable substrates, from liquids to soft solids. *Soft Matter* **8,** 7177–7184 (2012).

28. Nadermann, N., Hui, C.-Y. & Jagota, A. Solid surface tension measured by a liquid drop under a solid film. *Proc. Natl. Acad. Sci.* **110,** 10541–10545 (2013).

29. Drelich, J., Miller, J. D. & Good, R. J. The effect of drop (bubble) size on advancing and receding contact angles for heterogeneous and rough solid surfaces as observed with sessile-drop and captive-bubble techniques. *J. Colloid Interface Sci.* **179,** 37–50 (1996).

30. Drelich, J. The effect of drop (bubble) size on contact angle at solid surfaces. *J. Adhes.* **63,** 31–51 (1997).

31. Drelich, J. & Miller, J. D. The effect of surface heterogeneity on pseudo-line tension and the flotation limit of fine particles. *Colloids and Surfaces* **69,** 35–43 (1992).

32. Xu, Z. *et al.* Reversible hydrophobic to hydrophilic transition in graphene via water splitting induced by UV irradiation. *Sci. Rep.* **4,** 6450 (2015).

33. Russo, C. J. & Passmore, L. A. Controlling protein adsorption on graphene for cryo-EM using low-energy hydrogen plasmas. *Nat. Methods* **11,** 649–652 (2014).

34. Jiang, L., Fu, W., Birdja, Y. Y., Koper, M. T. M. & Schneider, G. F. Quantum and electrochemical interplays in hydrogenated graphene. *Nat. Commun.* **9,** 793 (2018).

35. Mcevoy, N., Nolan, H., Nanjundan, A. K., Hallam, T. & Duesberg, G. Functionalization of graphene surfaces with downstream plasma treatments. *Carbon N. Y.* **54,** 283–290 (2013).

36. Driskill, J., Vanzo, D., Bratko, D. & Luzar, A. Wetting transparency of graphene in water. *J. Chem. Phys.* **141,** 18C517 (2014).

37. Greenspan, L. Humidity fixed points of binary saturated aqueous solutions. *J. Res. Natl. Bur. Stand. Sect. A Phys. Chem.* **81A,** 89 (1977).

38. Huang, P. Y. *et al.* Grains and grain boundaries in single-layer graphene atomic patchwork quilts. *Nature* **469,** 389–392 (2011).

39. Yu, Q. *et al.* Control and characterization of individual grains and grain boundaries in graphene grown by chemical vapour deposition. *Nat. Mater.* **10,** 443–449 (2011).

40. Lima, L. M. C., Arjmandi-Tash, H. & Schneider, G. F. Lateral non-covalent clamping of graphene at the edges using a lipid scaffold. *ACS Appl. Mater. Interfaces* **10,** 11328–11332 (2018).

41. Andrews, J. E., Sinha, S., Chung, P. W. & Das, S. Wetting dynamics of a water nanodrop on graphene. *Phys. Chem. Chem. Phys.* **18,** 23482–23493 (2016).

42. Sakae Suzuki, Peter G. Green, R. E. B. & Siddharth Dasgupta, William A. Goddard Ill, G. A. B. Benzene forms hydrogen bonds with water. **257,** 942–944 (1992).

43. Gierszal, K. P. *et al.* π-hydrogen bonding in liquid water. *J. Phys. Chem. Lett.* **2,** 2930–2933 (2011).

44. Bepete, G. *et al.* Surfactant-free single-layer graphene in water. *Nat. Chem.* **9,** 347–352 (2016).

45. Ricardo, K. B., Sendecki, A. & Liu, H. Surfactant-free exfoliation of graphite in aqueous solutions. *Chem. Commun.* **50,** 2751–2754 (2014).